JACS
JOURNAL OF THE AMERICAN CHEMICAL SOCIETY
Article
pubs.acs.org/JACS

An Insight into the Mechanism of the Axial Ligand Exchange Reaction in Boron Subphthalocyanine Macrocycles

Julia Guilleme,[†] Lara Martínez-Fernández,[‡] David González-Rodríguez,*[,†] Inés Corral,*[,‡] Manuel Yáñez,[‡] and Tomás Torres*[,†,§]

[†]Departamento de Química Orgánica, Facultad de Ciencias, Universidad Autónoma de Madrid, Cantoblanco, 28049 Madrid, Spain
[‡]Departamento de Química, Facultad de Ciencias, Universidad Autónoma de Madrid, Cantoblanco, 28049 Madrid, Spain
[§]IMDEA Nanociencia, c/Faraday 9, Campus de Cantoblanco, 28049 Madrid, Spain

Supporting Information

ABSTRACT: We provide here an insight into the mechanism of the axial ligand exchange reaction between chlorosubphthalocyanines and phenols. Our combined experimental and theoretical results support a bimolecular σ-bond metathesis mechanism in which the phenolic proton assists in weakening the boron−halogen bond concomitantly with substitution at the boron center. Such a reaction pathway, which is unusual in boron chemistry, is a consequence of the crowded and rigid chemical environment of the boron atom in these macrocycles. Furthermore, this work sheds light on the influence of different experimental parameters on the kinetics and efficiency of the most important reaction in subphthalocyanine chemistry.

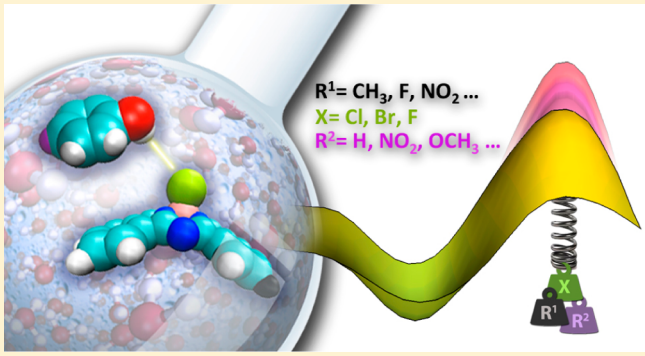

INTRODUCTION

Forty years after their discovery, subphthalocyanines (SubPcs) (Figure 1)[1] have meritedly found their own place within the domain of π-conjugated molecules with valuable optoelectronic properties. This smaller version of the phthalocyanine (Pc)[2] macrocycle, comprising three isoindole units instead of four, has demonstrated great potential in different applied fields.[1] Most of the technological interest in these molecules comes from their singular cone-shaped 14-π-electron aromatic structure, their strong absorption in the visible region (550−600 nm), and their adjustable electronic properties. They were originally investigated as promising dyes for nonlinear optical (NLO) applications because of the possibility of combining strong dipolar and octupolar contributions.[3] Their low tendency to aggregate in solution, due to their nonplanar structure, has also motivated their use in photodynamic therapy (PDT).[4] On the other hand, these molecules with easily tailored redox properties and excited states can act as efficient energy/electron donors or acceptors in artificial photosynthesis mimics.[5] Industrial interest has also arisen in view of the possibility of employing these purple-magenta dyes as inks or in optical recording media.[6] Furthermore, in the last years, numerous reports have highlighted the potential of SubPcs as active components in optoelectronic devices such as organic field-effect transistors (OFETs),[7] organic light-emitting diodes (OLEDs),[8] and organic photovoltaic cells (OPVs).[9,10]

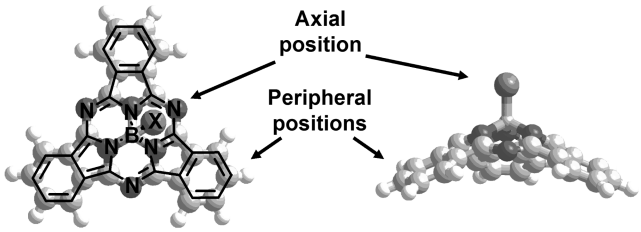

Figure 1. Top and side views of the structure of SubPc (X = axial ligand).

SubPcs are only known to date as boron complexes. The small boron atom fits perfectly into the SubPc central cavity and efficiently templates the phthalonitrile cyclotrimerization reaction that leads to these macrocycles. This synthetic process is typically carried out in the presence of a boron trihalide (BCl_3 or BBr_3) at high temperatures.[1,11] As a result, a halide atom (Cl or Br) ultimately occupies the axial position of the SubPc.

The reactivity at the axial boron−halogen bond in SubPcs has been exhaustively employed for the derivatization of these molecules for different purposes. First of all, axial functionalization can assist in solubilizing these molecules in water[4b,12] or organic[13] media, which is essential for biological applications or device processing. On the other hand, it has been demonstrated that substitution with less labile axial ligands increases their thermal, optical, and chemical stability.[13,14] Besides, this substitution site allows for the straightforward incorporation

Received: August 9, 2014
Published: September 11, 2014

   dx.doi.org/10.1021/ja508181b | J. Am. Chem. Soc. 2014, 136, 14289−14298

of SubPcs into larger multicomponent systems without affecting the electronic properties of the macrocycle, which are mainly determined by the nature of the peripheral substituents.[5a] Phenols are by far the most commonly employed reagents for these axial substitution reactions. A recent survey demonstrated that more than 90% of the research published in chemistry journals on SubPcs during the last 10 years involves the synthesis of phenoxy-SubPcs.[11b] The main reason, besides the ones mentioned above, is that the reaction with phenol derivatives is simple and straightforward and affords moderate to good yields in general.[1,11]

Despite the central importance and the expediency of this particular synthetic protocol, very little is known about the axial substitution mechanism in haloboron SubPcs. The tetracoordinated boron atom in these SubPc precursors is relatively inert since the vacant *p* orbital is occupied by the formation of a dative bond with one of the nitrogens in the macrocycle. As a result, boron SubPcs enjoy a singular, intriguing reactivity very different from that of common boron halides.[15] For instance, experimental evidence has shown that phenols and carboxylic acids react faster with haloboron SubPcs than alkyl alcohols or amines, despite their lower nucleophilicity,[16] and that these compounds can undergo axial halide exchange reactions in the presence of a Lewis acid such as BF_3[17] or $AlCl_3$.[18] This evidence seems to imply a transition state in which the B−X bond is considerably weakened before actual nucleophilic attack. With this idea in mind, some synthetic strategies have already been developed that generate activated electrophilic SubPc intermediates[19] for axial ligand exchange reactions.[18,20] Because of the frequent use and importance of this reaction in the chemistry of subazamacrocycles as well as the unusual characteristics of the boron atom confined in a rigid tritopic cavity, we were determined to gain a deeper understanding of the actual axial substitution mechanism. We report here our combined experimental and theoretical results that support a bimolecular σ-bond metathesis mechanism in which the phenolic proton assists in weakening the B−Cl bond concurrently with substitution at the boron center.

RESULTS AND DISCUSSION

Kinetic Measurements. Reaction Rate Order Determination. The model axial ligand exchange reaction studied in this work is shown in Scheme 1. It involves the substitution of the halogen atom in haloboron SubPcs with a phenoxy ligand by heating a solution of the two reagents. Our kinetic measurements focused on the effect of concentration, solvent, and reagent structure (R^1 and R^2 groups) on the reaction rate before 10% conversion. The reaction progress was monitored by taking aliquots at given times and quantifying reagent and product relative concentrations by HPLC. The experimental HPLC conditions and a typical set of chromatograms taken during reaction progress (Figure S2) can be found in the Supporting Information (SI).

First of all, we were interested in ascertaining the initial rate order for each reagent and hence the molecularity of the reaction. We chose a standard reaction between trimethylchloro-SubPc (**S1**) and 4-*tert*-butylphenol (**P1**)[21] in toluene at 100 °C (Scheme 1). Several mechanisms were considered in which the reaction followed first-, second-, or third-order rate laws.[22] Among them, the most chemically relevant (shown in Figure 2) are the following:

(i) The reaction follows a first-order rate law that is dependent only on the SubPc (**S**) concentration. This would imply a mechanism in which the B−X bond is dissociated unimolecularly in the rate-determining step, after which fast nucleophilic attack by the phenol (**P**) occurs. Under these conditions, the following relationships must hold:

$$v = k[\mathbf{S}]$$

$$\ln[\mathbf{S}] = \ln[\mathbf{S}]_0 - kt$$

(ii) The reaction follows a second-order rate law that also depends on the phenol concentration, meaning that both species participate in the transition state of the rate-determining step. If this is the case, the following relationships must hold:

$$v = k[\mathbf{S}][\mathbf{P}]$$

Scheme 1. Model Axial Ligand Exchange Reaction between Haloboron SubPcs (S1−S9) and Phenols (P1−P5)

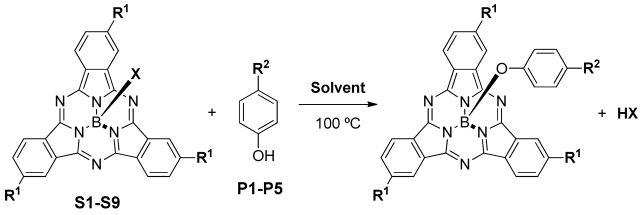

S1	$R^1 = CH_3$	X = Cl	**P1**	$R^2 = t$Bu
S2	$R^1 = CH_3$	X = Br	**P2**	$R^2 = OCH_3$
S3	$R^1 = CH_3$	X = F	**P3**	$R^2 = H$
S4	$R^1 = F$	X = Cl	**P4**	$R^2 = I$
S5	$R^1 = F$	X = Br	**P5**	$R^2 = NO_2$
S6	$R^1 = OCH_3$	X = Cl		
S7	$R^1 = OPh$	X = Cl		
S8	$R^1 = I$	X = Cl		
S9	$R^1 = NO_2$	X = Cl		

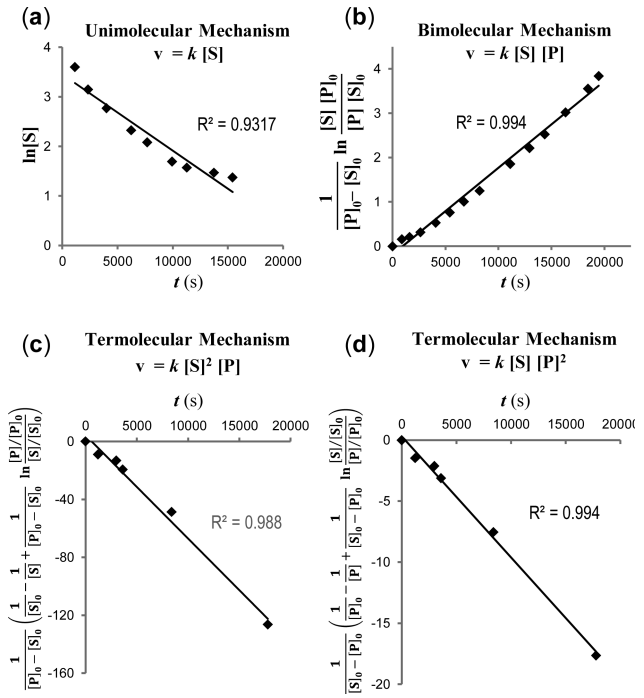

Figure 2. Fits of the kinetic data in the standard reaction between **S1** and **P1** to (a) first-order, (b) second-order, and (c, d) third-order rate laws. In all cases, the following conditions were used: $[\mathbf{S1}]_0 = 2.5 \times 10^{-2}$ M; $[\mathbf{P1}]_0 = 1.6 \times 10^{-1}$ M; $T = 100$ °C; toluene as the solvent.

dx.doi.org/10.1021/ja508181b | J. Am. Chem. Soc. 2014, 136, 14289−14298

$$\frac{1}{[\mathbf{P}]_0 - [\mathbf{S}]_0} \ln \frac{[\mathbf{S}][\mathbf{P}]_0}{[\mathbf{P}][\mathbf{S}]_0} = kt$$

(iii) Two phenol molecules and one SubPc molecule (or two SubPc molecules and one phenol molecule) participate in the transition state of the rate-controlling step. For two phenols and one SubPc, the following relationships must hold:

$$v = k[\mathbf{S}][\mathbf{P}]^2$$

$$\left(\frac{1}{[\mathbf{S}]_0 - [\mathbf{P}]_0}\right)\left(\frac{1}{[\mathbf{P}]} - \frac{1}{[\mathbf{P}]_0} + \frac{1}{[\mathbf{S}]_0 - [\mathbf{P}]_0} \ln \frac{[\mathbf{P}][\mathbf{S}]_0}{[\mathbf{S}][\mathbf{P}]_0}\right) = kt$$

The equations for the case of two SubPcs and one phenol are analogous.

It is interesting to note the analogy between the first two proposed mechanisms and the mechanisms of nucleophilic substitution on sp^3 carbon atoms (S_N1 and S_N2).[22] The outcome of our experiments revealed that *the reaction progress at low conversions reliably fits a bimolecular second-order rate law* of the type $v = k$[SubPc][ArOH] that is dependent on both the SubPc and phenol concentrations, while the first- and third-order equations do not fit the experimental data. It should be noted that this statement applies to all the kinetic measurements performed in this work, no matter the concentration, the solvent, or the nature of the SubPc and ArOH reagents employed.

These results were perfectly reproducible at different SubPc or phenol initial concentrations. As shown in Figure 3, we obtained in all cases kinetic data that fit the second-order rate law, from which we could derive the rate constants. The reaction rate *increases with SubPc concentration* at constant phenol concentration and *increases with phenol concentration* at constant SubPc concentration. On the other hand, the addition of a base such as triethylamine or pyridine, which can sequester the HCl released during the reaction,[4a,20,23] did not produce any kinetic effect at low conversions. We noticed nonetheless that they help in leading this reversible reaction to completion.[24]

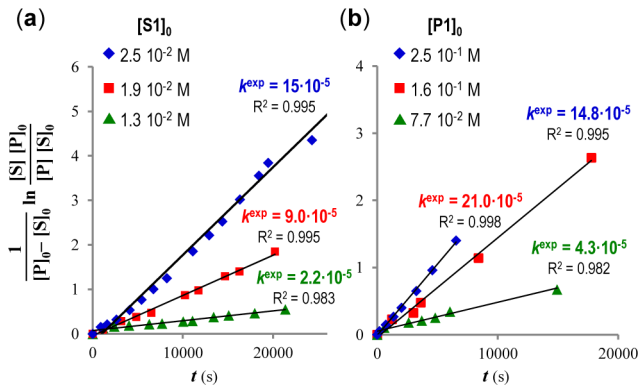

Figure 3. Influence of the SubPc and phenol concentrations on the axial substitution rate. Shown are fits of the kinetic data for the reaction between **S1** and **P1** in toluene at 100 °C to a second-order rate law at (a) different **S1** initial concentrations (with $[\mathbf{P1}]_0 = 1.6 \times 10^{-1}$ M) and (b) different **P1** initial concentrations (with $[\mathbf{S1}]_0 = 2.5 \times 10^{-2}$ M).

One may notice that the good fit of the data in Figure 2d might point to a third-order rate law. However, this would imply that two molecules of phenol and one molecule of SubPc react in the transition state, which is far more unlikely than the bimolecular process. Nonetheless, in order to rule out this possibility, we estimated the partial reaction orders with respect to SubPc and phenol from the experimental results shown in Figure 3, in which the concentration of one of the reagents was varied while the other was maintained constant. Considering a general reaction rate law of the type:

$$v = k[\mathbf{S}]^m[\mathbf{P}]^n$$

and applying the initial rate method, we could determine that $m = 1$ and $n = 1$ (see the SI). In other words, when the initial SubPc concentration was doubled (or tripled) while the phenol concentration was kept constant, the initial rate was alongside doubled (or tripled), and the same held when only the initial concentration of phenol was changed.

Theoretical Insight into the Reaction Mechanism. Our theoretical mapping of the reaction mechanism investigated by means of density functional theory (DFT) supports the bimolecular second-order rate law predicted by the kinetic experiments. Figure 4 shows a postulated double-well reaction profile for the axial substitution reaction of chloro-SubPc using phenol as the nucleophile. The two reagents ($Reac_1$) approach and interact to form a prereaction complex ($Reac_2$) that then undergoes the transformation to products through a bimolecular transition state (TS). A postreaction complex ($Prod_2$) is then formed that dissociates into the final products, phenoxy-SubPc and HCl ($Prod_1$).

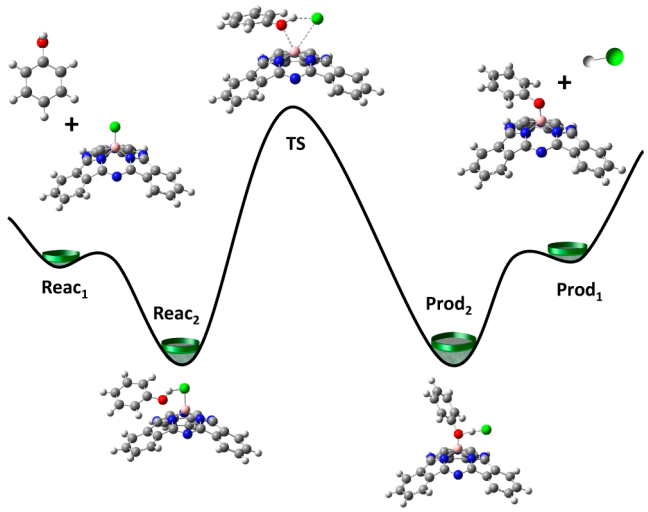

Figure 4. Double-well reaction profile postulated from DFT calculations for the substitution reaction between phenol and chloro-SubPc.

The phenol nucleophile approaching the SubPc substrate to reach the $Reac_2$ minimum could in principle attack the reaction center from the convex or concave side. In the first case, the reaction would proceed with retention of configuration, while the second case would require inversion of the SubPc bowl structure, in a similar fashion as for S_N2 reactions occurring at sp^3 C or B centers.[25] Since the Walden inversion products are not experimentally observed[26] because of the large amount of energy required to invert the bowl and the obvious steric effects, the concave attack was not theoretically explored.[27] Furthermore, we hypothesized that the establishment of hydrogen bonding between the phenolic proton and the chlorine atom would help anchor the phenol to the SubPc

dx.doi.org/10.1021/ja508181b | J. Am. Chem. Soc. 2014, 136, 14289−14298

($Reac_2$ complex), directing the nucleophilic attack and preparing the complex for the substitution reaction. This is supported by the electrostatic potential surface calculated for chloro-SubPc (Figure 5). The most prominent feature is the

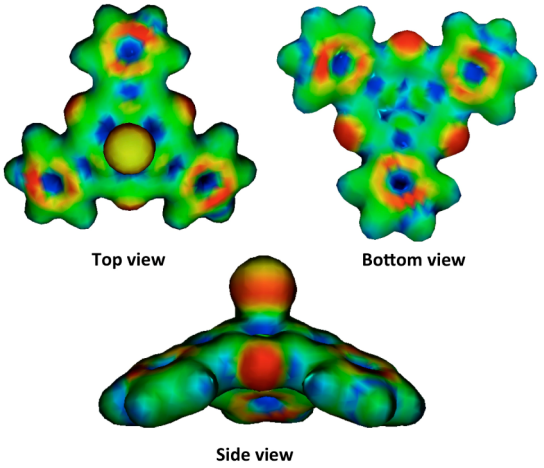

Figure 5. Electrostatic potential surface of chloro-SubPc calculated at the BLYP/def2-SVP level of theory.

negative potential (red regions) due to electron density accumulated around the chlorine atom, indicating the region of the substrate to which a proton would feel the strongest interaction.

As a matter of fact, our calculations indicate that all along the DFT-optimized double-well reaction profile, the phenol and the SubPc show strong interactions (hydrogen-bonding, van der Waals, electrostatic) and participate in all of the stationary points (i.e., th $Reac_2$ and $Prod_2$ minima and the central reaction barrier). These interactions were characterized using the atoms-in-molecules theory of Bader.[28] Topological analysis of the electron density revealed the positions of the bond critical points (BCPs) indicating the accumulation of electron density between pairs of bonded atoms. For a given pair of atoms, the electron density measured at the BCP can be taken as a good indicator of the strength of the linkage. The map of the line of maximum density between these two atoms would define the bond path. Then, molecular graphs were constructed from the scaffold of calculated BCPs and bond paths (Figure 6).[28]

Our calculations on the prereaction complex, $Reac_2$, confirm strong phenol−SubPc interactions (Figure 6b). The BCP localized between the Cl atom and the proton from the alcohol group supports the hydrogen-bonding hypothesis. An additional weak interaction between Cl and the ortho H atom of the phenol was also located. Moreover, the phenol nucleophile was found to interact with the SubPc via two additional weak van der Waals/electrostatic interactions involving the O and the ortho C atom of the phenol and two C atoms from a SubPc isoindole group. On the contrary, our calculations do not predict important interactions between the incoming phenolic O atom and the B substitution center, which is exclusively bonded to the Cl atom (Figure 6a).

As the substitution reaction progresses toward the TS with the approach of the phenol, the B−Cl bond experiences a significant stretching and deviation from the original SubPc vertical axis. This allows for a more parallel disposition of the two aromatic systems that strengthens their interaction, as reflected by the double electron densities computed at the C−

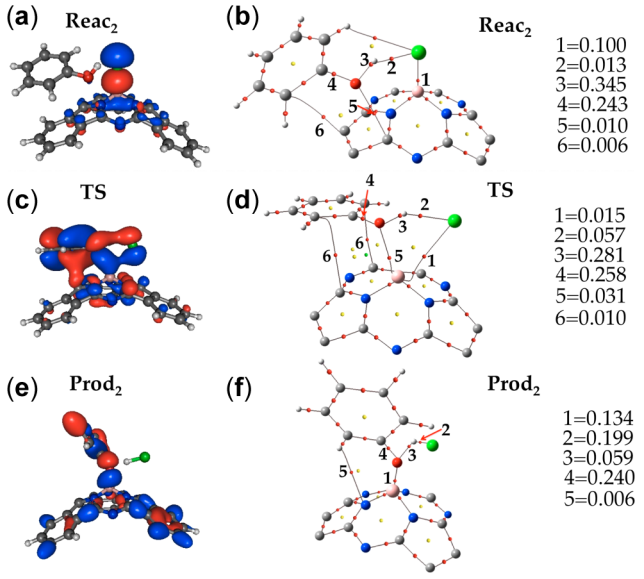

Figure 6. Molecular orbitals relevant for the description of (a, c, e) the bonding and (b, d, f) the molecular graphs around the reaction center of the stationary points localized along the reaction path for the axial substitution reaction. Bond critical points are shown in red, ring critical points in yellow, and cage critical points in green. Electron densities at the relevant critical points are given in e au^{-3}.

C-located BCPs relative to those of $Reac_2$ (compare Figure 6b and Figure 6d). In the TS, the reaction center develops a new BCP between the O of the phenol and the boron of the SubPc that was not present in $Reac_2$, leading to a four-center bond that accounts for the respective formation and breaking of the B−O and B−Cl bonds (see the molecular orbitals and graphs in Figure 6c,d). This $Reac_2$ → TS activation free energy governs the substitution reaction kinetics. Since the molecularity of this step in the mechanism is not changing (the two molecules are already bound in $Reac_2$), we believe that the major contribution to this transition is enthalpic, while the entropic term should be similar at the two stationary points.

The strengthening of the B−O bond in the postreaction complex $Prod_2$ (Figure 6f) forces a change in the orientation of the phenol and SubPc moieties, therefore minimizing their interaction. At this point, the substitution subproduct, HCl, is still interacting with the phenoxy-SubPc product via hydrogen bonding (Figure 6f).

Similar double-well profiles and interactions in the reaction center from $Reac_2$ and TS were found for other aliphatic nucleophiles considered (i.e., ethanol). The most significant difference found between these two pairs of reactions was in the intermolecular interactions, aside from the reaction center, which were found to be stronger in the case of phenol as a result of the aromatic nature of the two interacting moieties.

Factors Influencing the Reaction Kinetics. In order to get further insight in the mechanism and kinetics of this process, we made some modifications to the standard reaction (see Scheme 1) in order to determine the influence of the nature of the leaving halogen atom (X), the distribution of the electron density of the SubPc macrocycle as a function of the peripheral R^1 groups, and the nucleophilicity of the phenol (as determined by the *para* R^2 groups) on the substitution rate. The experimental findings have been rationalized in terms of both the geometrical changes and evolution of the interactions between the two reagents along the substitution reaction profile

dx.doi.org/10.1021/ja508181b | J. Am. Chem. Soc. 2014, 136, 14289−14298

and the encountered barrier height in the $Reac_2 \rightarrow TS$ transition.[29] All of them are key parameters to analyze substitution reactions.

Figures 7−9 collect the results of the kinetic experiments, computed DFT gas-phase relative energies (calculated as differences between electronic ground-state energies without including thermal corrections), and geometries for selected SubPcs and nucleophiles. These figures also show the experimentally fitted and theoretically estimated rate constants for comparison. See the SI for further details.

a. Nature of the Axial Halogen. It is known that the axial halogen atom has a strong influence on this substitution reaction, with bromo-SubPcs reacting faster and more efficiently than chloro-SubPcs.[30] This is indeed what we could determine quantitatively in our experiments. In order to compare the bromo and chloro leaving groups, we also had to modify the starting SubPc reagents to the trifluoro-SubPcs **S4** and **S5** because the corresponding trimethylbromo-SubPc **S2** was too reactive and difficult to purify as a result of fast hydrolysis of the B−Br bond. Nonetheless, the kinetic data obtained (Figure 7a) demonstrate that *a bromine leaving atom reacts 3 orders of magnitude faster than chlorine*. On the other hand, the chloro and fluoro leaving groups were also compared in the trimethyl-substituted SubPcs **S1** and **S3**. Our results indicate that *chloro-SubPcs react much faster than fluoro-SubPcs*, which were inert under our standard conditions.

Theoretical insight into the effect of the nature of the axial halogen on the kinetics of the substitution reaction was obtained by comparing the energy barriers calculated for the F-, Cl-, and Br-substituted SubPcs (**S3**, **S4**, and **S5**, respectively; see Figure 7b). The associated computed energy barriers amount to 200, 170, and 154 kJ/mol, leading correspondingly to rate constants of 3.4×10^{-11}, 2×10^{-5}, and 324×10^{-5} M^{-1} s^{-1}. The value for **S5** perfectly matches the experimentally fitted rate constant, but the experimental and theoretical rate constants differ by an order of magnitude for **S4**. Such a difference, however, would reflect an underestimation of the calculated energy barrier by only 6 kJ/mol. On the other hand, the high barrier estimated for the F-substituted SubPc is in agreement with the lack of reactivity observed experimentally for **S3**.

This reactivity trend (Br > Cl > F) can be rationalized in terms of the different geometric changes experienced by the bond being broken (B−X) and the bond being formed (B−O) in moving from $Reac_1$ to $Reac_2$ and then to the TS. The B−X distances in the starting SubPcs were computed to 1.39 Å (B−F), 1.90 Å (B−Cl), and 2.20 Å (B−Br), thus increasing in the order *F* < Cl < Br, as expected according to the atomic radii of the halogens.[31] On the contrary, the structural evolution from $Reac_1$ to the TS demands a B−X stretching that follows the inverse order: 1.25 Å (B−F), 1.10 Å (B−Cl), and 0.76 Å (B−Br). This means that the TS in the reaction of bromo-SubPc **S5** and **P3** is structurally related to the reagents, while in the other extreme, the TS in the reaction of fluoro-SubPc **S3** and **P3** closely resembles the products. Chloro-SubPc **S4** represents an intermediate case. Further analysis confirms these hypotheses. The B−O distance (which decreases in moving from $Reac_2$ to TS) is ca. 0.5 Å longer for **S5** than for **S4** or **S3** at the TS, while the H−F bond distance for **S3** is computed to be 1.033 Å at the TS, which is very close to the H−F gas-phase equilibrium distance, suggesting almost complete transfer of the proton to the F atom. These observations are in accordance with the Hammond postulate, which states that the TS most resembles

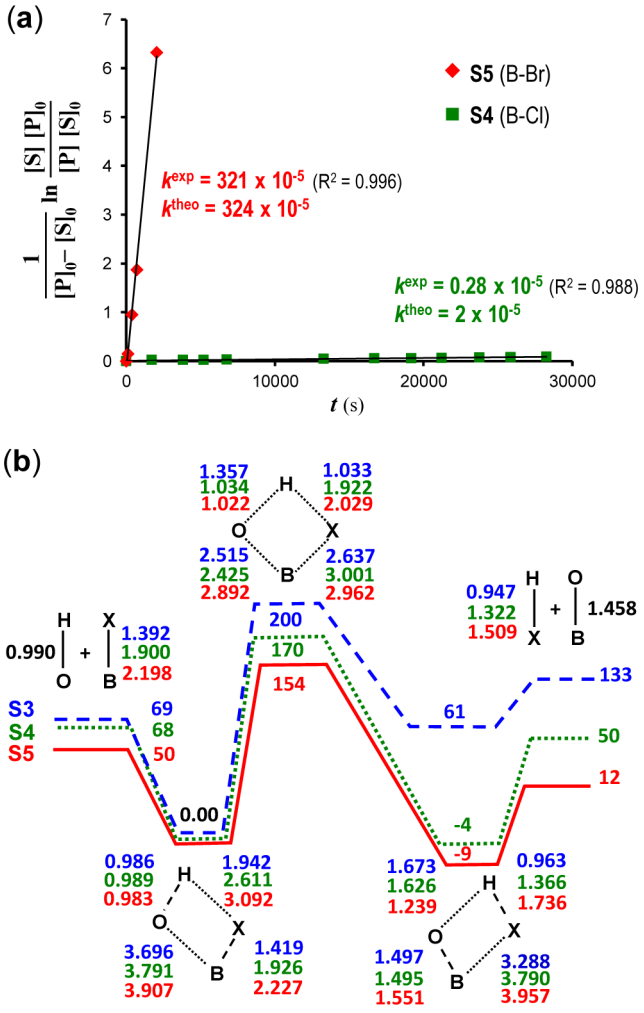

Figure 7. Influence of the axial halogen atom on the substitution rate. (a) Fits of the kinetic data to a second-order rate law and theoretically estimated rate constants in the reactions between **S4** or **S5** and **P1**. In all cases, the following conditions were used: $[S]_0 = 2.5 \times 10^{-2}$ M; $[P]_0 = 1.6 \times 10^{-1}$ M; T = 100 °C; toluene as the solvent. (b) Energetics (in kJ/mol) of the substitution reactions for **S3**, **S4**, and **S5** and important distances (in Å) regarding the reaction centers.

the adjacent reactant/product to which it is closest in energy, and would explain the reactivity trends observed for these SubPc reagents.

A closer look at the specific stabilizing interactions established both in the prereaction minima $Reac_2$ and in the TSs of these systems reveal further information along the same line as the structural analysis performed above to explain the computed energy barriers and experimental reactivity trends. Our calculations show that the van der Waals/electrostatic interactions between the nucleophile and the substrate in going from the initial complex to the TS become more important in the order **S3** < **S4** < **S5** (see Figure S3 in the SI). In other words, for **S3** the interactions between the two aromatic moieties weaken along the $Reac_2 \rightarrow TS$ transition (see Figure S3), while for **S4** the encounter complex maintains such interactions. In the case of **S5**, these interactions become more important at the TS. In fact, whereas for F- and Cl-SubPc the phenol moiety experiences a slight rotation to become parallel to the SubPc ring upon reaching the TS, in the case of Br-SubPc the phenol moves from a perpendicular position to a

dx.doi.org/10.1021/ja508181b | J. Am. Chem. Soc. 2014, 136, 14289−14298

parallel position relative to the SubPc moiety (see Figure S3). These observations are consistent with the computed dissociation energies for the three reactions ($Reac_1$ energies; Figure 7b), which decrease in the order F ≈ Cl (ca. 70 kJ mol^{-1}) > Br (50 kJ mol^{-1}).

b. Effect of Peripheral Substitution. The effect of the peripheral substituents (R^1 in Scheme 1) on the reaction rate was then quantitatively evaluated. These substituents, which are directly bound at the isoindole rings, are known to rule the electron density of the macrocycle,[5a] and theoretical calculations have revealed that they also have an influence on the length and polar character of the axial B−X bond.[32] Six different chloro-SubPcs were targeted, equipped with three peripheral R^1 groups of diverse electronic nature: −OMe (**S6**), −OPh (**S7**), −Me (**S1**), −I (**S8**), −F (**S4**), and $-NO_2$ (**S9**). However, compound **S6** (R^1 = OMe) was discarded from these experiments since, like bromo-SubPc **S2** mentioned above, the isolation of pure starting chloro-SubPc material was not simple because of fast hydrolysis of the B−Cl bond. This always led to a small amount of hydroxy-SubPc in the starting material, which hampered obtaining reliable kinetic data. The results obtained for the other five starting reagents (Figure 8a) reveal that *SubPcs substituted with electron-donating groups react faster than those substituted with electron-withdrawing groups.* The influence of the peripheral groups on the axial substitution rate is very significant. For instance, a comparison between SubPcs **S1** and **S8** indicated that the reaction proceeds 2 orders of magnitude faster with the former reagent. As an extreme case, trinitro-SubPc **S9** was not even reactive under our standard reaction conditions: it took several days to start detecting traces of product.

Rationalization of the effect of the peripheral substituents on the reaction rate can be achieved by comparing the reaction barriers calculated for the methoxy- (**S6**), methyl- (**S1**), fluoro- (**S4**), and nitro- substituted (**S9**) chloro-SubPcs. As expected on the basis of the longer distance of these substituents from the reaction center, the differences found between the computed reaction barriers for these systems are subtler than for the SubPcs differing in the axial substituent discussed above. However, an analysis in terms of geometric changes in the $Reac_1 \rightarrow Reac_2 \rightarrow TS$ pathway and the evolution of the intermolecular interactions between the two moieties similar to the one presented above can be done in order to explain the different kinetic behavior of these SubPcs.

A first issue to be noticed from our calculations is that the nature of the peripheral substituents has some effect on the remote B−Cl bond. In line with previous studies,[32] the computed B−Cl distance slightly increases in the order R^1 = NO_2 < F < CH_3 in ca. 0.01 Å increments (Figure 8b). The distance change is small, but the trend is clear and is reproduced in $Reac_1$, $Reac_2$, and the TS. It has been interpreted in terms of the rearrangement of the electron density of the substituted macrocycle, which has an effect on the length and ionic character of the B−X bond. This trend in the polarity of the B−X bond is also evident from the examination of the electrostatic potential surfaces calculated for SubPcs **S1**, **S4**, **S6**, and **S9**. In fact, **S9** presents the most electrophilic B atom, that is, it shows the most positive and least negative electrostatic potentials at the B and Cl positions, respectively, while for **S6** the opposite is found (Figure S6b in the SI). Aside from the B−X lengthening in SubPcs with electron-donating peripheral groups, which is in accordance with their higher reactivities, we observed again that higher energy barriers are found for TSs

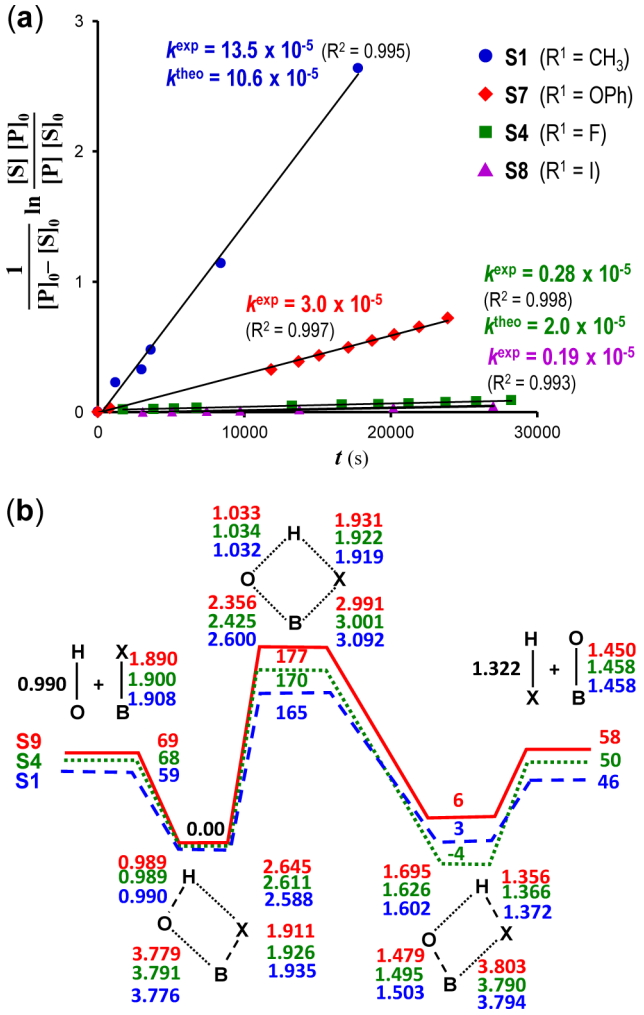

Figure 8. Influence of the SubPc peripheral substitution on the substitution rate. (a) Fits of the kinetic data to a second-order rate law and theoretically estimated rate constants in the reactions between **S1**, **S7**, **S4**, or **S8** and **P1**. In all cases, the following conditions were used: $[S]_0 = 2.5 \times 10^{-2}$ M; $[P]_0 = 1.6 \times 10^{-1}$ M; T = 100 °C; toluene as the solvent. (b) Energetics (in kJ/mol) of the substitution reactions for **S1**, **S4**, and **S9** and important distances (in Å) regarding the reaction centers.

that are structurally closer to the products. For instance, the B−O distances at the TS increase in the order 2.36 Å (R^1 = NO_2) < 2.42 Å (R^1 = F) < 2.60 Å (R^1 = CH_3) as the donor character of the substituent increases (Figure 8b). Once more, the difference in the stabilizing interactions established between one of the SubPc isoindole moieties and the phenol nucleophile at the $Reac_2$ and TS geometries would complement the previous explanation regarding the influence of R^1 on the barrier height. While these interactions are similar for all of the TSs considered, they are especially stronger at the position of $Reac_2$ for electron-deficient macrocycles (i.e., **S9** and **S4**; see the molecular graphs in Figure S4 in the SI). As a result of the overstabilization of the $Reac_2$ minima for NO_2- and F-SubPc, the barrier heights leading to the substitution products through the TS become larger.

c. Nature of the Nucleophile. Furthermore, we observed that the nature of the phenol reagent also has an enormous effect on the reaction rate (Figure 9a). A comparison among phenols **P1**−**P5** in the reaction with **S1** led to the conclusion

dx.doi.org/10.1021/ja508181b | J. Am. Chem. Soc. 2014, 136, 14289−14298

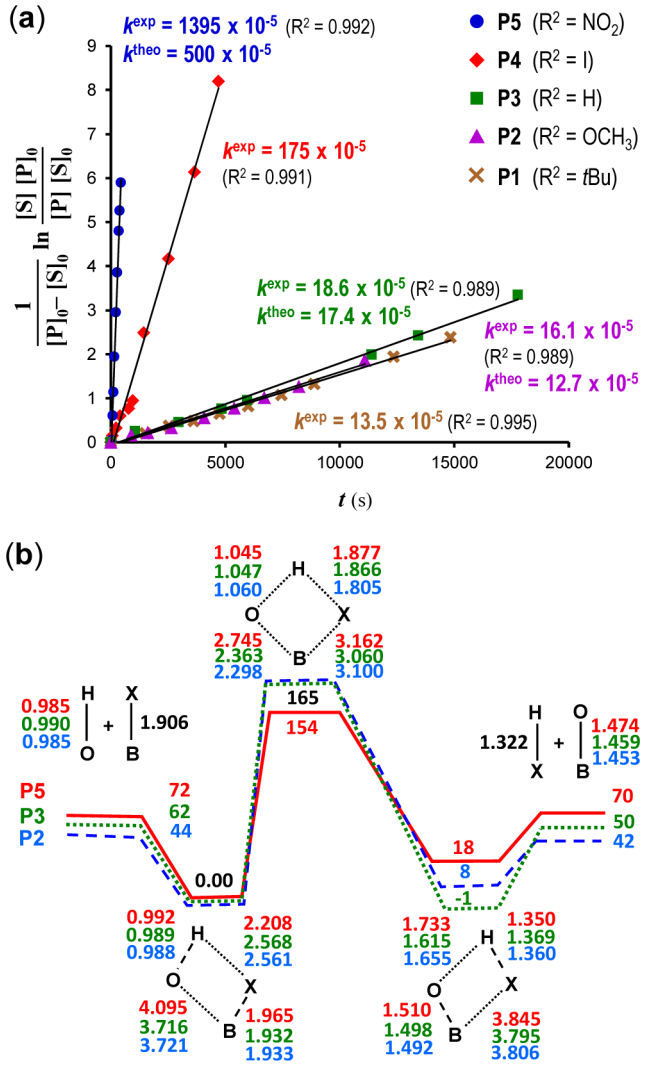

Figure 9. (a) Influence of the phenol R^2 group on the axial substitution rate. (a) Fits of the kinetic data to a second-order rate law in the reactions between **S1** and **P1**–**P5**. In all cases, the following conditions were used: $[S]_0 = 2.5 \times 10^{-2}$ M; $[P]_0 = 1.6 \times 10^{-1}$ M; T = 100 °C; toluene as the solvent. (b) Energetics (in kJ/mol) of the substitution reactions for **P2**, **P3**, and **P5** and important distances (in Å) regarding the reaction centers.

that *phenols having an electron-withdrawing group at the para position react much faster than phenols with an electron-donor group*. In other words, in order to increase the reaction rate, one must not make the phenol more nucleophilic with electron-donating groups; rather, it must be made more acidic with electron-withdrawing groups. For instance, 4-nitrophenol (**P5**) showed very fast conversion under our standard conditions: it reacted 2 orders of magnitude faster than unsubstituted phenol (**P3**). A Hammett plot was built from the kinetic data obtained for the five phenols (Figure 10a). We observed a linear correlation between the Hammett σ parameter of the substituent at the para position and the $\log(k/k_H)$ term, where k_H is the rate constant of the reference unsubstituted phenol **P3**. From this fit, a positive moderate ρ parameter (ρ = 2.11) was derived.

This last observation is remarkable. It implies that the nucleophile strength is not an important factor in accelerating the axial substitution reaction. On the contrary, our results further support the hypothesis that the phenolic proton plays

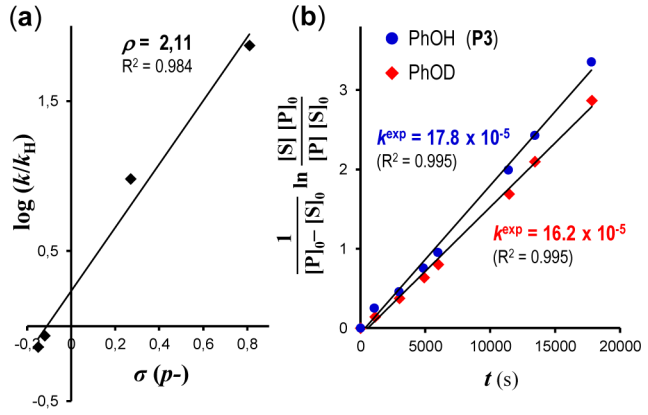

Figure 10. (a) Hammett correlation between the σ parameter and $\log(k/k_H)$ for the four para-substituted phenols. (b) Influence of isotopic labeling on the axial substitution rate. Shown are fits of the kinetic data to a second-order rate law in the reactions between **S1** and PhOD or PhOH (**P3**) in toluene.

an important role in the transition state of the rate-determining step through coordination to the axial halogen and assistance in the dissociation of the B–X bond. In order to shed more light on this theory, kinetic isotope effects were evaluated as well (Figure 10b).[33] The k_H/k_D ratios obtained with deuterated and nondeuterated phenols in toluene at 100 °C are certainly not large (k_H/k_D = 1.15), but they are measurable and reproducible. Such low primary isotope effect values could be interpreted as a contradiction of our assumption that the phenolic proton participates at the TS of the axial exchange reaction. However, the reason for this low value can be found in the origin of primary isotope effects. Our calculations presume nonlinear TSs having O–H–X angles that are not far from 90°. When H/D transfer proceeds through an activated complex with bent bonds, bending modes become important. Since the force constants for scissoring and bending motions are substantially lower than those for stretching motions, the zero-point energy differences between the reactant and activated complexes are not as large as for reactions involving H/D transfer through linear TSs. This is manifested in primary kinetic isotope effects of much lower magnitude.[34]

On the other hand, our theoretical findings are again in line with the experimental observations. We observed an energy barrier 11 kJ/mol larger for **P2** and **P3** (R^2 = OCH_3 and H, respectively) than for **P5** (R^2 = NO_2), and consistently, a 40 times larger kinetic constant was calculated for **P5** (Figure 9b). It is interesting to remark the shortening experienced by the H–X bond along the $Reac_2$ → TS pathway as a function of the nature of the phenol: 0.76 Å (R^2 = OCH_3) > 0.70 Å (R^2 = H) > 0.33 Å (R^2 = NO_2). According to the Hammond principle, the greater resemblance of the H–X distances in the TS and $Reac_2$ in **P5** and in the TS and $Prod_2$ in **P2** and **P3** would explain the lower energy barrier in the former case. In line with this trend, the B–O bond distance in $Reac_2$ increases in the order 3.71 Å (R^2 = H) ≈ 3.72 Å (R^2 = OCH_3) < 4.10 Å (R^2 = NO_2) as the electron-withdrawing character of the substituent increases (Figure 9b). Interestingly, although **P5** is still far from the reaction center at the $Reac_2$ minimum, it presents the most stretched B–Cl distance, leading to the complex most prepared to undergo the substitution reaction (Figure 9b).

The previous values derived for the B–O distance at $Reac_2$ can be rationalized in terms of the intermolecular interactions between the phenol and SubPc moieties. Although these

dx.doi.org/10.1021/ja508181b | J. Am. Chem. Soc. 2014, 136, 14289–14298

interactions are similar to the ones found for **S9** (please recall the previous section), in **P5** they produce a remarkable distancing between the phenol O atom and the B atom. This prevents the establishment of a stabilizing electrostatic interaction between the two atoms, thereby reducing the energy barrier between the prereaction complex $Reac_2$ and the TS. These interactions do exist when R^2 = H or OCH_3, as the B−O distance is ca. 0.3 Å shorter compared with that in the NO_2-substituted nucleophile (Figure 9b and Figure S5 in the SI).

d. Solvent Effects. Finally, the kinetic effects of solvent coordination power (CP)[35] and polarity (measured as a function of the dielectric constant, ε)[36] were also considered as a relevant tool to gather additional experimental evidence. On one hand, we compared the rates of the standard reaction between **S1** and **P1** at 100 °C in aromatic, weakly coordinating solvents such as toluene (ε = 2.38), *o*-dichlorobenzene (ε = 9.93), benzonitrile (ε = 26.0), and nitrobenzene (ε = 34.82) in order to assess the effect of solvent polarity. The observed experimental trend is that *solvents of increasing polarity induce a faster axial substitution reaction*. For instance, as illustrated in Figure 11a, the reaction proceeds 1 order of magnitude faster in nitrobenzene than in toluene. However, *the use of polar coordinating solvents results on the contrary in lower reaction rates*. That is the case for DMF (ε = 36.7; CP = 0.72[35a]) where the reaction is considerably slower than in toluene (Figure 11a). In 1,4-dioxane, which is both coordinating and nonpolar, our standard reaction was slower than in toluene. These solvent effects suggest that a polar environment is beneficial for a fast ligand exchange reaction as long as the solvent does not strongly compete with the interaction between the phenol and the Cl atom in the transition state (Figure 11b).

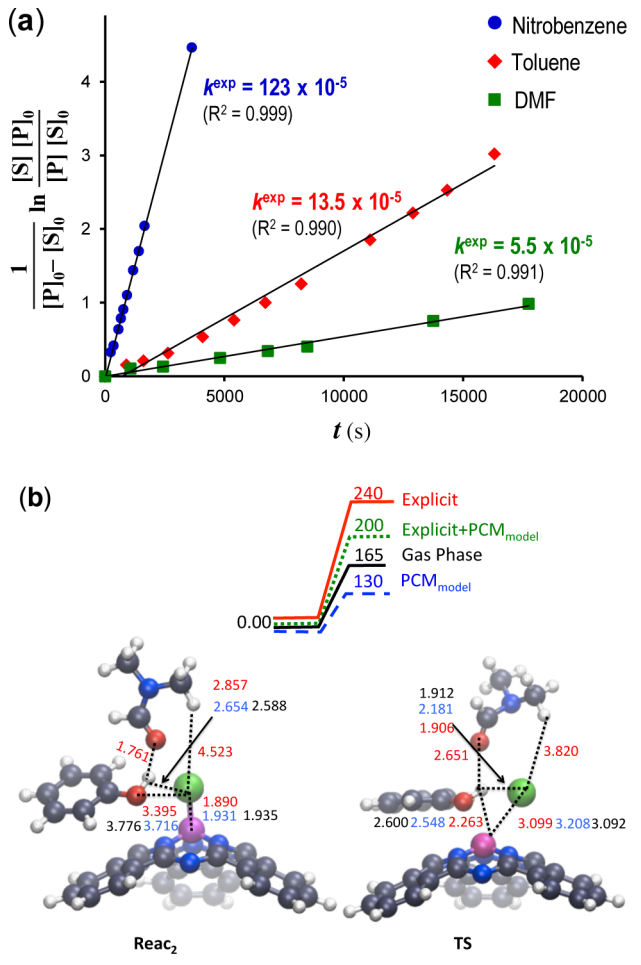

Figure 11. Influence of the solvent environment on axial substitution rate. (a) Fits of the kinetic data to a second-order rate law in the reactions between **S1** and **P1** in nitrobenzene, toluene, and DMF. In all cases, the following conditions were used: $[S]_0 = 2.5 \times 10^{-2}$ M; $[P]_0 = 1.6 \times 10^{-1}$ M; T = 100 °C. (b) Energetics (in kJ/mol) and stationary points optimized for the substitution reactions considering implicit and explicit DMF molecules.

In order to analyze the role of solvent polarity in the kinetics of the substitution reaction in SubPc, we investigated the reaction profiles including the effect of toluene and nitrobenzene solvents. No kinetic constants were calculated in these cases, since the pre-exponential factor is known to be strongly affected by solvent effects, but a qualitative analysis of their influence on the energy barriers could still be done. In agreement with the experimental observations, in going from toluene to nitrobenzene the TS is stabilized by 22 kJ/mol, which can be explained by the significantly charged nature of the TS.

The coordination power of the solvent was also investigated from a theoretical point of view using DMF as in the experiments. When the solvent molecules were considered only implicitly, the energy barrier for the optimized TS was calculated to amount to 130 kJ/mol, just the same as the value computed for nitrobenzene, since the two solvents are characterized by very similar dielectric constants. However, a dramatic change in the energy barrier, which increased to 239 kJ/mol, was observed when an explicit solvent molecule was introduced into our calculations (Figure 11b). This barrier, however, translates into a much a smaller kinetic constant than the one found experimentally. Interestingly, in the simulation of both the solvent coordination and the solvent polarity, the two effects act in opposite directions, increasing and decreasing the energy barrier, respectively. This leads to an intermediate energy barrier of 200 kJ/mol, in line with the experimentally fitted reaction rate constant.

Conclusions: Postulated Mechanism. In view of all these experimental and theoretical results, we propose an *associative metathesis mechanism* in which two σ bonds (B−X and O−H) are broken and two new σ bonds (B−O and H−X) are formed concertedly at the TS of the rate-controlling step (Figure 12).

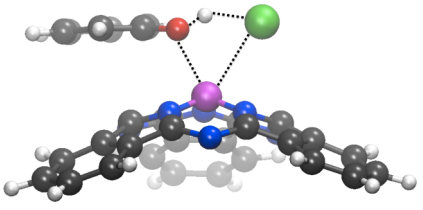

Figure 12. Proposed TS structure of the rate-controlling step in the axial substitution reaction between chloro-SubPcB and phenol, indicating an associative σ-bond metathesis mechanism.

In other words, we propose that the phenol assists in the dissociation of the polar boron−halogen bond by proton coordination while the new B−O bond is being formed. This would explain the following observations: (1) the reaction is bimolecular, with a rate depending on both the SubPc and phenol concentrations; (2) bromo-SubPcs react faster than chloro and fluoroSubPcs, since the boron−halogen bond is

dx.doi.org/10.1021/ja508181b | J. Am. Chem. Soc. 2014, 136, 14289−14298

longer and weaker in that series; (3) SubPcs substituted with electron-donating groups at the periphery react faster as a result of the stabilization of the positive charge developed at the B atom in the transition state; (4) more acidic phenols accelerate the reaction, since they are able to bind more efficiently to the leaving halogen atom via proton coordination; (5) the obtained Hammett ρ parameter is positive, which points to stabilization of the partial negative charge generated at the O atom in the TS by electron-withdrawing groups; (6) the measured kinetic isotope effect values are low, which would indicate that the extent of O−H dissociation is not large and, especially, that the activated complex has a bent O−H−X bond; (7) non-coordinating solvents with a high dielectric constant induce a faster reaction, since they can stabilize the partial charges generated in the transition state; and (8) solvents that can compete with the phenol to form hydrogen bonds, as in the case of DMF or dioxane, lead to reduced reactivity.

This σ-bond metathesis mechanism also explains several other SubPc axial exchange reactions reported in the literature. For instance, it supports the notion that aromatic alcohols and even carboxylic acids react much faster than aliphatic alcohols.[26] This may be the case because, despite their lower nucleophilicity, more acidic protons would stabilize the TS more efficiently by coordination to the halide, as shown in this work. A similar mechanism would also explain the reactivity of Lewis acid reagents (boron or aluminum trihalides, trimethylsilyl derivatives, etc.) in axial exchange reactions. The Lewis acidic center may coordinate to the axial halogen in a similar way as a proton, thereby weakening the B−X bond in tandem with the formation of the new B−Y bond.

We have also shown in this work that previous to the TS, important interactions are generated in the $Reac_2$ complex between the phenol and isoindole aromatic surfaces that bring together the two reagents. An interesting issue that could be further addressed is a comparison of the reactivities of subazaporphyrin (SubPz), SubPc, and subnaphthalocyanine (SubNc) with phenol nucleophiles. It has been empirically observed[17] that axial halogen exchange reactions are more efficient in the order SubPz > SubPc > SubNc, but the origin behind this reactivity difference has not yet been disclosed. Likewise, a comparison of the reactivities of the structurally related SubPz and subporphyrin (SubP) macrocycles would also be an appealing issue to study. The higher stability of the SubP ring may allow other reaction pathways to occur.

In conclusion, this work sheds light on the influence of different experimental parameters on the kinetics and efficiency of the most important reaction in SubPc chemistry. Moreover, our work describes a reaction mechanism that is, to the best of our knowledge, unprecedented in boron chemistry and arises as a consequence of the crowded and rigid chemical environment of the boron atom in these singular macrocycles.

■ ASSOCIATED CONTENT

Supporting Information

Experimental procedures, compound characterization data, and Figures S1−S6. This material is available free of charge via the Internet at http://pubs.acs.org.

■ AUTHOR INFORMATION

Corresponding Authors

david.gonzalez.rodriguez@uam.es
ines.corral@uam.es
tomas.torres@uam.es.

Notes

The authors declare no competing financial interest.

■ ACKNOWLEDGMENTS

Funding from MINECO (MAT2012-38538-CO3-01 and -02 and CTQ2012-31914), MICINN and MEC [F.P.U. fellowships (J.G. and L.M.-F.), CTQ-2011-24187/BQU, CTQ2011-23659, CTQ2012-35513-C02-01 is gratefully acknowledged. Generous allocation of computational time from the Centro de Computación Científica UAM is gratefully acknowledged. The authors thank J. M. Segovia for the design of the graphical abstract.

■ REFERENCES

(1) (a) Claessens, C. G.; González-Rodríguez, D.; Torres, T. *Chem. Rev.* **2002**, *102*, 835−853. (b) Claessens, C. G.; González-Rodríguez, D.; Rodríguez-Morgade, M. S.; Medima, A.; Torres, T. *Chem. Rev.* **2014**, *114*, 2192−2277.

(2) *Handbook of Porphyrin Science*; Kadish, K. M., Smith, K. M., Guilard, R., Eds.; World Scientific: Singapore, 2010; Vols. *1*−*15*.

(3) (a) del Rey, B.; Keller, U.; Torres, T.; Rojo, G.; Agulló-López, F.; Nonell, S.; Marti, C.; Brasselet, S.; Ledoux, I.; Zyss, J. *J. Am. Chem. Soc.* **1998**, *120*, 12808−12817. (b) Claessens, C. G.; González-Rodríguez, D.; Torres, T.; Martín, G.; Agulló-López, F.; Ledoux, I.; Zyss, J.; Ferro, V. R.; García de la Vega, J. M. *J. Phys. Chem. B* **2005**, *109*, 3800−3806.

(4) (a) Xu, H.; Jiang, X.-J.; Chan, E. Y. M.; Fong, W.-P; Ng, D. K. P. *Org. Biomol. Chem.* **2007**, *5*, 3987−3992. (b) Spesia, M. B.; Durantini, E. N. *Dyes Pigm.* **2008**, *77*, 229−237.

(5) (a) González-Rodríguez, D.; Torres, T.; Guldi, D. M.; Rivera, J.; Herranz, M. A.; Echegoyen, L. *J. Am. Chem. Soc.* **2004**, *126*, 6301−6313. (b) González-Rodríguez, D.; Claessens, C. G.; Torres, T.; Liu, S.-G.; Echegoyen, L.; Vila, N.; Nonell, S. *Chem.—Eur. J.* **2005**, *11*, 3881−3893. (c) González-Rodríguez, D.; Torres, T.; Olmstead, M. M.; Rivera, J.; Herranz, M. A.; Echegoyen, L.; Atienza-Castellanos, C.; Guldi, D. M. *J. Am. Chem. Soc.* **2006**, *128*, 10680−10681. (d) González-Rodríguez, D.; Torres, T.; Herranz, M. A.; Echegoyen, L.; Carbonell, E.; Guldi, D. M. *Chem.—Eur. J.* **2008**, *14*, 7670−7679. (e) El-Khouly, M. E.; Shim, S. H.; Araki, Y.; Ito, O.; Kay, K.-Y. *J. Phys. Chem. B* **2008**, *112*, 3910−3917. (f) González-Rodríguez, D.; Carbonell, E.; Guldi, D. M.; Torres, T. *Angew. Chem., Int. Ed.* **2009**, *48*, 8032−8036. (g) El-Khouly, M. E.; Ryu, J. B.; Kay, K.-Y.; Ito, O.; Fukuzumi, S. *J. Phys. Chem. C* **2009**, *113*, 15444−15453. (h) González-Rodríguez, D.; Carbonell, E.; de Miguel Rojas, G.; Atienza Castellanos, C.; Guldi, D. M.; Torres, T. *J. Am. Chem. Soc.* **2010**, *132*, 16488−16500. (i) El-Khouly, M. E.; Ju, D. K.; Kay, K.-Y.; D'Souza, F.; Fukuzumi, S. *Chem.—Eur. J.* **2010**, *16*, 6193−6202. (j) Romero Nieto, C.; Guilleme, J.; Villegas, C.; Delgado, J. L.; González-Rodríguez, D.; Martín, M.; Torres, T.; Guldi, D. M. *J. Mater. Chem.* **2011**, *21*, 15914−15918. (k) Romero-Nieto, C.; Medina, A.; Molina-Ontoria, A.; Claessens, C. G.; Echegoyen, L.; Martín, N.; Torres, T.; Guldi, D. M. *Chem. Commun.* **2012**, *48*, 4953−4955. (l) El-Khouly, M. E.; Kim, J.-H.; Kim, J.-H.; Kay, K.-Y.; Fukuzumi, S. *J. Phys. Chem. C* **2012**, *116*, 19709−19717. (m) Romero-Nieto, C.; Guilleme, J.; Fernández-Ariza, J.; Rodríguez-Morgade, M. S.; González-Rodríguez, D.; Torres, T.; Guldi, D. M. *Org. Lett.* **2012**, *14*, 5656−5659.

(6) (a) Wang, Y.; Gu, D.; Gan, F. *Phys. Status Solidi* **2001**, *186*, 71−77. (b) For related patents, see ref 1.

(7) (a) Renshaw, C. K.; Xu, X.; Forrest, S. R. *Org. Electron.* **2010**, *11*, 175−178. (b) Tong, X.; Forrest, S. R. *Org. Electron.* **2011**, *12*, 1822−1825.

(8) (a) Chen, Y.-H.; Chang, J.-H.; Lee, G.-R.; Wu, I.-W.; Fang, J.-H.; Wu, C.-I.; Pi, T.-W. *Appl. Phys. Lett.* **2009**, *95*, No. 133302. (b) Morse, G. E.; Helander, M. G.; Maka, J. F.; Lu, Z.-H.; Bender, T. P. *ACS Appl. Mater. Interfaces* **2010**, *2*, 1934−1944. (c) Helander, M. G.; Morse, G. E.; Qiu, J.; Castrucci, J. S.; Bender, T. P.; Lu, Z.-H. *ACS Appl. Mater. Interfaces* **2010**, *2*, 3147−3152. (d) Morse, G. E.; Castrucci, J. S.;

Helander, M. G.; Lu, Z.-H.; Bender, T. P. *ACS Appl. Mater. Interfaces* **2011**, *3*, 3538−3544.
(9) (a) Mutolo, K. L.; Mayo, E. I.; Rand, B. P.; Forrest, S. R.; Thompson, M. E. *J. Am. Chem. Soc.* **2006**, *128*, 8108−8109. (b) Gommans, H.; Cheyns, D.; Aernouts, T.; Girotto, C.; Poortmans, J.; Heremans, P. *Adv. Funct. Mater.* **2007**, *17*, 2653−2658. (c) Gommans, H.; Schols, S.; Kadashchuk, A.; Heremans, P.; Meskers, S. C. J. *J. Phys. Chem. C* **2009**, *113*, 2974−2979. (d) Verreet, B.; Schols, S.; Cheyns, D.; Rand, B. P.; Gommans, H.; Aernouts, T.; Heremans, P.; Genoe, J. *J. Mater. Chem.* **2009**, *19*, 5295−5297. (e) Gommans, H.; Aernouts, T.; Verreet, B.; Heremans, P.; Medina, A.; Claessens, C. G.; Torres, T. *Adv. Funct. Mater.* **2009**, *19*, 3435−3439. (f) Pegg, L.-J.; Schumann, S.; Hatton, R. A. *ACS Nano* **2010**, *4*, 5671−5678. (g) Mauldin, C. E.; Piliego, C.; Poulsen, D.; Unruh, D. A.; Woo, C.; Ma, B.; Mynar, J. L.; Fréchet, J. M. J. *ACS Appl. Mater. Interfaces* **2010**, *2*, 2833−2838. (h) Verreet, B.; Rand, B. P.; Cheyns, D.; Hadipour, A.; Aernouts, T.; Heremans, P.; Medina, A.; Claessens, C. G.; Torres, T. *Adv. Energy Mater.* **2011**, *1*, 565−568. (i) Cho, S. W.; Piper, L. F. J.; DeMasi, A.; Preston, A. R. H.; Smith, K. E.; Chauhan, K. V.; Sullivan, P.; Hatton, R. A.; Jones, T. S. *J. Phys. Chem. C* **2010**, *114*, 1928−1933. (j) Girotto, C.; Voroshazi, E.; Cheyns, D.; Heremans, P.; Rand, B. P. *ACS Appl. Mater. Interfaces* **2011**, *3*, 3244−3247. (k) Kim, J. Y.; Noh, S.; Nam, Y. M.; Kim, J. Y.; Roh, J.; Park, M.; Amsden, J. J.; Yoon, D. Y.; Lee, C.; Jo, W. H. *ACS Appl. Mater. Interfaces* **2011**, *3*, 4279−4285. (l) Wang, N.; Zimmerman, J. D.; Tong, X.; Xiao, X.; Yu, J.; Forrest, S. R. *Appl. Phys. Lett.* **2012**, *101*, No. 133901. (m) Menke, S. M.; Luhman, W. A.; Holmes, R. J. *Nat. Mater.* **2012**, *12*, 152−157. (n) Beaumont, N.; Cho, S. W.; Sullivan, P.; Newby, D.; Smith, K. E.; Jones, T. S. *Adv. Funct. Mater.* **2012**, *22*, 561−566. (o) Verreet, B.; Cnops, K.; Cheyns, D.; Heremans, P.; Stesmans, A.; Zango, G.; Claessens, C. G.; Torres, T.; Rand, B. P. *Adv. Energy Mater.* **2014**, DOI: 10.1002aenm.201301413. (p) Cnops, K.; Rand, B. P.; Cheyns, D.; Verreet, B.; Empl, M. A.; Heremans, P. *Nat. Commun.* **2014**, *5*, No. 3406.
(10) A recent overview of this connection highlights these advances. See: Morse, G. E.; Bender, T. P. *ACS Appl. Mater. Interfaces* **2012**, *4*, 5055−5068.
(11) Claessens, C. G.; González-Rodríguez, D.; del Rey, B.; Torres, T.; Mark, G.; Schuchmann, H.-P.; von Sonntag, C.; MacDonald, J. G.; Nohr, R. S. *Eur. J. Org. Chem.* **2003**, 2547−2551.
(12) (a) Xu, H.; Ng, D. K. P. *Chem.—Asian J.* **2009**, *4*, 104−110. (b) Lapok, L.; Claessens, C. G.; Wöhrle, D.; Torres, T. *Tetrahedron Lett.* **2009**, *50*, 2041−2044.
(13) Brisson, E. R. L.; Paton, A. S.; Morse, G. E.; Bender, T. P. *Ind. Eng. Chem. Res.* **2011**, *50*, 10910−10917.
(14) (a) González-Rodríguez, D.; Torres, T.; Denardin, E. L. G.; Samios, D.; Stefani, V.; Corrêa, D. S. *J. Organomet. Chem.* **2009**, *694*, 1617−1622. (b) Yamasaki, Y.; Mori, T. *Chem. Lett.* **2010**, *39*, 1108−1109. (c) Samdal, S.; Volden, H. V.; Ferro, V. R.; Garcia de la Vega, J. M.; Gonzalez-Rodriguez, D.; Torres, T. *J. Phys. Chem. A* **2007**, *111*, 4542−4550.
(15) *Contemporary Aspects of Boron: Chemistry and Biological Applications*; Ali, H. A., Dembitsky, V. M., Srebnik, M., Eds.; Elsevier: Amsterdam, 2005.
(16) Potz, R.; Göldner, M.; Hückstädt, H.; Cornelissen, U.; Tutaß, A.; Homborg, H. *Z. Anorg. Allg. Chem.* **2000**, *626*, 588−596.
(17) Rodríguez-Morgade, M. S.; Claessens, C. G.; Medina, A.; González-Rodríguez, D.; Gutierrez-Puebla, E.; Monge, A.; Alkorta, I.; Elguero, J.; Torres, T. *Chem.—Eur. J.* **2008**, *14*, 1342−1350.
(18) Morse, G. E.; Bender, T. P. *Inorg. Chem.* **2012**, *51*, 6460−6467.
(19) Kato, T.; Tham, F. S.; Boyd, P. D. W.; Redd, C. A. *Heteroat. Chem.* **2006**, *17*, 209−216.
(20) Guilleme, J.; González-Rodríguez, D.; Torres, T. *Angew. Chem., Int. Ed.* **2011**, *50*, 3506−3509.
(21) For practical reasons, a small excess of phenol with respect to the SubPc (6.4 equiv) was generally employed in this standard reaction.
(22) Anslyn, E. V.; Dougherty, D. A. *Modern Physical Organic Chemistry*; University Science Books: Sausalito, CA, 2006.
(23) (a) Liu, J.-Y.; Yeung, H.-S.; Xu, W.; Li, X.; Ng, D. K. P. *Org. Lett.* **2008**, *10*, 5421−5424. (b) Shibata, N.; Das, B.; Tokunaga, E.; Shiro, M.; Kobayashi, N. *Chem.—Eur. J.* **2010**, *16*, 7554−7562. (c) Xu, H.; Ng, D. K. P. *Inorg. Chem.* **2008**, *47*, 7921−7927.
(24) When reaction conversion is high and the HCl is not eliminated, so that its concentration in solution is not negligible, some of the phenoxy-SubPc product can react with HCl to re-form the starting chloro-SubPc. Similar reactions between phenoxy-SubPcs and $AlCl_3$ have been observed (see ref 18). Thus, a base can help at high conversions by fully shifting this equilibrium to the formation of phenoxy-SubPc.
(25) Imamoto, T.; Morishita, H. *J. Am. Chem. Soc.* **2000**, *122*, 6329−6330.
(26) Unlike other bowl-shaped molecules such as cyclotriveratrilene, calixarene, sumanene, and corannulene, SubPcs are rigid macrocycles that do not undergo bowl inversion. In other words, it is known that these molecules, when resolved into their enantiomerically pure form, do not racemize. See: (a) Samdal, S.; Volden, H. V.; Ferro, V. R.; García de la Vega, J. M.; González-Rodríguez, D.; Torres, T. *J. Phys. Chem. A* **2007**, *111*, 4542−4550. (b) Shimizu, S.; Miura, A.; Khene, S.; Nyokong, T.; Kobayashi, N. *J. Am. Chem. Soc.* **2011**, *133*, 17322−17328.
(27) Other examples of substitution reactions on sp^3 C, Si, and P leading to unexpected stereoselectivity can also be found in the literature. For C and Si, see: Corriu, J. P. R.; Guerin, C. *J. Organomet. Chem.* **1980**, *198*, 231−320. For P, see: Zijlstra, H.; León, T.; de Cózar, A.; Guerra, C. F.; Byrom, D.; Riera, A.; Verdaguer, X.; Bickelhaupt, F. M. *J. Am. Chem. Soc.* **2013**, *135*, 4483−4491. In all of these works, the generation of the unconventional product is justified by the establishment of stabilizing interactions in prereaction encounter complexes involving the nucleophile and the substrate that favor the nonexpected attacking pathway for either thermodynamic or steric reasons.
(28) Bader, R. F. W. *Atoms in Molecules: A Quantum Theory*; Clarendon Press: Oxford, U.K., 1990.
(29) To facilitate the discussion, the absolute energy of $Reac_2$ was taken as the zero of energy. Energies presented throughout the text are therefore relative to the $Reac_2$ minima.
(30) (a) Fulford, M. V.; Jaidka, D.; Paton, A. S.; Morse, G. E.; Brisson, E. R. L.; Lough, A. J.; Bender, T. P. *J. Chem. Eng. Data* **2012**, *57*, 2756−2765. (b) Paton, A. S.; Morse, G. E.; Castelino, D.; Bender, T. P. *J. Org. Chem.* **2012**, *77*, 2531−2536.
(31) These B−X distance values closely match those obtained by X-ray diffraction for unsubstituted SubPcs: 1.39 Å (B−F), 1.86 Å (B−Cl), and 2.05 Å (B−Br). See ref 1.
(32) (a) Ferro, V. R.; García de la Vega, J. M.; González-Jonte, R. H.; Poveda, L. A. *THEOCHEM* **2001**, *537*, 223−234. (b) Ferro, V. R.; Poveda, L. A.; Claessens, C. G.; González-Jonte, R. H.; García de la Vega, J. M. *Int. J. Quantum Chem.* **2003**, *91*, 369−375.
(33) Melander, L.; Saunders, W. A., Jr. *Reaction Rates of Isotopic Molecules*; John Wiley & Sons: New York, 1980.
(34) (a) More O'Ferrall, R. A. *J. Chem. Soc. B* **1970**, 785−790. (b) Vitale, A. A.; San Filippo, J., Jr. *J. Am. Chem. Soc.* **1982**, *104*, 7341−7343. (c) Anhede, B.; Bergman, N.-A. *J. Am. Chem. Soc.* **1984**, *106*, 7634−7636.
(35) (a) Munakata, M.; Kitagawa, S.; Miyazima, M. *Inorg. Chem.* **1985**, *24*, 1638−1643. (b) Munakata, M.; Kitagawa, S. *Inorg. Chim. Acta* **1990**, *169*, 225−234.
(36) Although they do not accurately represent solvent polarity, the reported dielectric constant values have been taken in this work as an approximation of the qualitative classification of polar solvents.